IEEE Access
Multidisciplinary ⋮ Rapid Review ⋮ Open Access Journal

Advanced Fault Detection, Classification, and Localization in Transmission Lines: A Comparative Study of ANFIS, Neural Networks, and Hybrid Methods

Shazia Kanwal[1], *Student Member, IEEE,* and Somchat Jiriwibhakorn[1], *Member, IEEE*
[1]School of Engineering, King Mongkut's Institute of Technology Ladkrabang (KMITL), Bangkok 10520, Thailand

Corresponding author: Somchat Jiriwibhakorn (somchat.ji@kmitl.ac.th).

ABSTRACT Electric systems are getting more complex with time, and primitive protection methods such as traveling wave and impedance-based methods face limitations and shortcomings. This paper incorporates and presents the applications of an adaptive neuro-fuzzy inference system and compares it with a back propagation neural network, self-organizing map, and hybrid method of discrete wavelet with adaptive neuro-fuzzy inference system for fault detections, classification, and localization in transmission lines. These methods, in comparison with primitive methods, could be capable of detecting, identifying, and predicting the location of the faults more accurately. The IEEE 9-bus system is utilized to obtain data from one end of the transmission line to develop an ANFIS-based model. This system is simulated in MATLAB/Simulink for different fault cases at various locations. The three-phase voltage and current at one end of IEEE 9-bus number seven are taken for training. Three ANFIS models are developed for fault detection, classification, and localization and compared with other models. For verification of the models, mean square error, mean absolute error, and regression analysis have been computed and compared for all the models. All four techniques have performed well for fault classification, detection, and location. However, the percentage error for the ANFIS-based fault model is less compared to backpropagation, self-organizing map, and discrete wavelet transform with ANFIS. Therefore, the proposed ANFIS models can be implemented for deploying in real-time-based protection systems.

INDEX TERMS ANFIS, SOM, DWT Fault Detection, Classification and Location, IEEE-9 Bus System, Transmission Line.

I. INTRODUCTION

THE three stages of the power system are generation, transmission, and distribution. The electrical system is built to provide stable and continuous electricity [2]. Some parts of electrical systems are exposed to the environment, so these systems are more susceptible to faults. There are two main types of faults in transmission lines: short circuit faults or shunt faults and series faults or open conductor faults. A fault in transmission lines is an undesirable event that may happen due to lightning, a short circuit between transmission lines, an accident, any other unforeseen incident, or even human error [1].

The short circuit faults in transmission lines are symmetrical and asymmetrical. Asymmetrical faults are single-line-to-ground, double-line, and double-line-to-ground faults. These faults are commonly known as phase A to ground (A-G), phase B to ground (B-G), phase C to ground (C-G), phase A to phase B (A-B), phase B to phase C (B-C), phase C to phase A (C-A), phase AB to ground (AB-G), phase BC to ground (BC-G), phase CA to ground (CA-G) faults. These faults cause instability in the power supply and severe damage to the system and humans [2]. Locating faults quickly and accurately is vital to reduce the outage time and save the system from major damage. Intelligent fault detection, identification, and Location will increase the electrical system's reliability, restore the power system, and reduce the power system's outage time [1],[3].

Protecting a transmission line uses relays at both ends that continuously monitor voltages and currents and respond to a fault. The most frequently utilized transmission line protection method is distance protection, with a line safety of around 85% [4].

There are a few limitations in using phasor-based methods in the protection system. First, delay associated with relay operation results in uncertainty in voltage protection. Second, to ensure quick tripping from both ends, it is necessary to employ a communication link between the relays at the two ends of the line [5]. Relay communication links provide a cyber threat when relays are connected to substation local area networks (LANs).

Researchers have presented several methods for transmission line fault detection and location methods; the broader categories are mentioned here: Conventional methods, Signal processing-based methods, and Artificial intelligence-based methods.

The conventional methods that are often used for the detection, classification, and localization of the fault in a transmission line are the traveling wave method and the impedance measurement-based method [6]. Single-end or two-end impedance techniques are suggested based on a variation of current and voltage signals gathered from a transmission line

terminal. Due to the high fault impedance, load on the line, source characteristics, and shunt capacitance, the fault location error of the impedance-based method is high [7].

To calculate the fault's distance, the traveling wave-based method compares the forward and backward propagation of waves in a transmission line. This approach is more accurate in finding faults in high resistance faults. However, the challenges are the high sampling frequency, high cost, and computational complexity that make practical use difficult [8].

Signal processing methods such as fast Fourier transform (FFT), wavelet transform (WT), multiresolution analysis (MRA), and discrete wavelet transform are some of the famous methods. WT is entirely accurate and can identify the fault characteristics using a faulty waveform's decomposed frequency components [9]. For the calculation of coefficients to be proper and precise, the FFT needs the signal to be stationary in the broad sense. However, most signals in power systems are flexible and fluctuate over time concerning their properties [4].

To address several issues with Fourier transform analysis techniques, multiresolution analysis (MRA), a signal processing tool, was established in the nineties [8], [4].

The discrete variant of the wavelet transform (WT), known as the discrete wavelet transform (DWT), is widely used to analyze discrete or sampled signals. The demand for DWT techniques in digital relaying systems has been rising recently in an era of digital communication and analysis [10].

For the safety of transmission lines, different AI-based fault detection, classification, and Location techniques, such as ANN, Fuzzy logic, and hybrid algorithms using integrated wavelet transform ANN, SVM, and fuzzy logic, have been used for the past few years [9], [15], [11].

Artificial neural networks, or ANNs, have traditionally been used successfully in various fault analysis studies. ANN's ability to learn independently is its most valuable feature.
The author in [11] suggested an ANN-based method in which a feed-forward neural network is used to detect and classify transmission line faults.

ANN is frequently combined with fuzzy logic inference to create an Adaptive Neuro-Fuzzy Inference System (ANFIS) topology, which many researchers have utilized to provide adequate security measures [12],[13],[14].

ANFIS is similar to a neural network, and the function is the same as a fuzzy inference system. ANFIS is used for the location and classification of faults in a transmission line. An adaptive network is a multilayer network where every node operates a particular function of the applied data set. The process of the node varies from node to node.

The author in [1] presented a neuro-fuzzy technique to investigate fault location estimates in power systems. The development of a 264 km, 132 kV, 50 Hz transmission line model and the simulation of various faults using MATLAB Simulink. To train the ANFIS, wavelet-processed data from both ends of the line are used, including the detailed features of the signal.

In contrast to other machine learning methods, the effectiveness of the Adaptive Neuro-Fuzzy Inference System (ANFIS) as an estimation model is discussed in [2]. In [14], to localize the fault site precisely, the method feeds the data into ANFIS and computes the line impedance using the approximation coefficients of these signals.

The use of an ANFIS and ANN for the classification and localization of faults in a lengthy transmission line is presented in [8]. Artificial intelligence-based machine learning techniques do better in specific tasks than other approaches. Using current and voltage data from the source end, ANFIS and ANN are used to precisely identify fault types and pinpoint the transmission line issue. Global System For Mobile Communication (GSM) and Global Positioning System (GPS) based ANN model has been developed in [16]. The challenge with such a communication-based protection system is that it could be more reliable, and there are always issues with cybersecurity threats.

Considering the mentioned restrictions, a new relaying technique is required. This technique helps the system operate without delay, just with currents and voltages, and without a communication link.

Therefore, this paper presents an Artificial Intelligence (AI) based technique that uses only voltage and current for fault detection, classification, and Location and is tested using only post-fault three-phase current and voltage.

The detection, classification, and localization of fault in a transmission line in an IEEE 9-bus system using ANFIS are studied in this paper. The post-fault three-phase voltage and current data from one end bus of an IEEE 9-bus system are used to detect and determine the fault's class and Location. All Asymmetrical marks are considered while varying the Location of the faults.
The main contributions in this paper are as follows:
1)The ANFIS-based technique is proposed for fault detection, classification, and Location, using one-end data for the IEEE 9 bus system.
2)IEEE has introduced a new technique called Self Organizing Map (SOM) for fault detection, classification, and location prediction.
3)Various asymmetrical faults under various conditions and for different Locations have been studied.
4)For the precision of the proposed ANFIS-based model, root mean square error, regression analysis, and mean absolute error are computed in MATLAB.
5)A comparison of the ANFIS-based model with a backpropagation neural network, self-organizing map, and discrete wavelet transform-based ANFIS is presented.
To present the mentioned goals, the paper is organized as follows. A brief overview of the system, the techniques ANFIS, ANN SOM, and DWT-ANFIS, and the detailed methodology are given in Section II. Simulation results for the proposed model for different fault conditions are given in Section III. And finally concluded in Section IV.

II. SYSTEM AND TECHNIQUES

A. SYSTEM STUDIED

The IEEE 9-bus system is used as a study model in this paper [17]. The single line diagram is given in Fig.1. All the data for the IEEE 9-bus system is taken from [18] and [19] and is

displayed in Fig. 2. The transmission line under study is between bus number 7 and bus number 8. The IEEE 9-bus system consists of three generators, three transformers, nine buses, six transmission lines, and three loads. The interconnection of all these utilities is shown in Fig. 2.

This system is simulated in MATLAB/Simulink version 2019a to implement the proposed ANFIS-based fault detection and classification technique.

B. PROPOSED TECHNIQUE

1) ADAPTIVE NEURO-FUZZY INFERENCE SYSTEM

ANFIS is a hybrid learning algorithm that best uses ANN and fuzzy logic. An adaptive network is a multilayer network where each node performs a specific function according to the applied data set. The process of each node is different from that of another node. This allows ANFIS to differentiate each input feature and detect the output.

Some advantages, such as better generalization ability, learning from experience, and better decision-making ability, make ANFIS better for complex problems. Therefore, ANFIS is helpful for fault detection, location, and classification in the transmission line. This approach has higher accuracy compared to other networks.

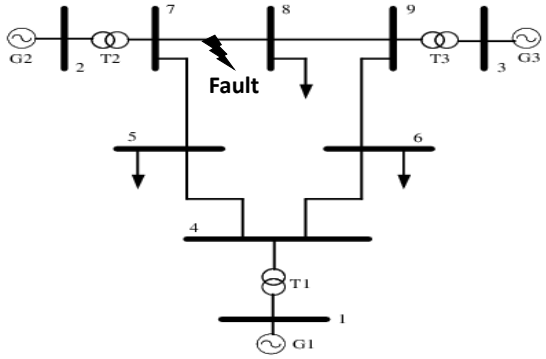

FIGURE 1. IEEE 9-bus system [17]

As mentioned above, a multilayer feedforward network called an adaptive network, shown in Fig.3, allows each node to perform a unique function on incoming signals and a set of parameters specific to that node. The node functions' formulae may differ from one node to the next, and the selection of each node function depends on the overall input-output function that the adaptive network must perform. It should be noted that connections in an adaptive network do not carry weights; instead, they simply represent the signal flow direction between nodes [20].

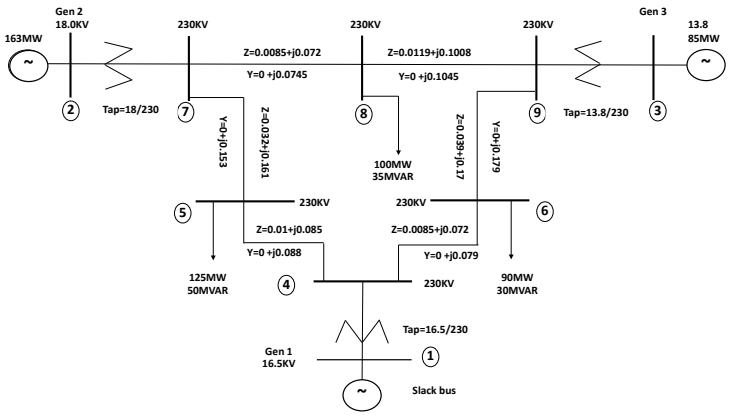

FIGURE 2. IEEE 9-bus system impedance diagram [18] [19].

As illustrated in Fig.3, the ANFIS construction includes a Fuzzy Interface System (FIS) whose membership function of parameters was altered using various methods, such as the backpropagation algorithm or the least squared approach. Compared to fuzzy inference systems, which are not offered by all fuzzy system possibilities, ANFIS is significantly more sophisticated. ANFIS exclusively supports the Sugeno-type and has a number of features that are compatible with the ANFIS system.

The mathematical structure of an Adaptive Neuro-fuzzy inference system with one prediction (output) y and two inputs x_1(current) and x_2 (voltage) is defined below [6][13].

The rule base has two Takagi and Sugeno-type fuzzy if-then rules.

Rule I: If x_1 is A_1 and x_2 is B_1, then $f_1 = p_1x_1 + q_1x_2 + r_1$.

Rule 2: If x_1 is A_2 and x_2 is B_2, then $f_2 = p_2x_1 + q_2x_2 + r_2$.

The five layers of the ANFIS structure are as follows:

Layer 1:

Each node i in this layer has a node function. An adaptive node is present in this labeling. The fuzzy membership grade of the inputs is the layer's executed output and is represented as follows:

$$O_i^1 = \mu A_i(x) \quad (1)$$

Where A is the linguistic label connected to this node. O_i^1 is the membership function of $\mu A_i(x)$. Every MF (membership function) is changed according to the layer's parameter.

Layer 2:

The nodes are fixed, nodes with the symbol π, which denotes that they perform function as a multiplier. Each node in this layer multiplies the input signals to determine the firing strength of each rule before sending the result out. The equation is written as follows:

$$O_i^2 = w_i = \pi_{j=1}^{m} \mu A_i(x) \quad (2)$$

Layer 3:

The nodes in this layer are fixed nodes as well. The nodes marked with a N, as shown in Fig.3, indicate that the firing strength has been normalized from the preceding layer. The equation for this layer is represented as follows:

$$O_i^3 = \overline{w} = \frac{w_i}{w_1 + w_2} \quad (3)$$

Layer 4:
Each node in this layer is an adaptive node, and the output parameters are modified in this layer. The output, which combined the first-order polynomial with the normalized firing strength, was processed for each node in the layer. As a result, this layer's outputs are provided as follows:

$$O_i^4 = y_i = \overline{W_i} f_i = \overline{W_i}(p_i x_1 + q_i x_2 + r_i), i = 1,2,.. \quad (4)$$

Layer 5:
In this layer, all the inputs from the previous layer are summed together to get the predicted output. The total sum output is given by below equation:

$$O_1^5 = \sum_i y_i = \sum_i \overline{w_i} f_i = \overline{w_1}(p_1 x_1) + \overline{w_1}(q_1 x_2) + (\overline{w_1} r_1) + \overline{w_2}(p_2 x_2) + \overline{w_2}(q_2 x_2) + (\overline{w_2} r_2) \quad (5)$$

The succeeding parameters can be solved using a least squares technique in this final layer. The final equation can be written as:

$$y = [w_1 x_1 \;\; w_1 x_2 \;\; w_1 \;\; w_2 x_2 \;\; w_2] \begin{bmatrix} p_1 \\ q_1 \\ r_1 \\ p_2 \\ q_2 \\ r_2 \end{bmatrix} = XW \quad (6)$$

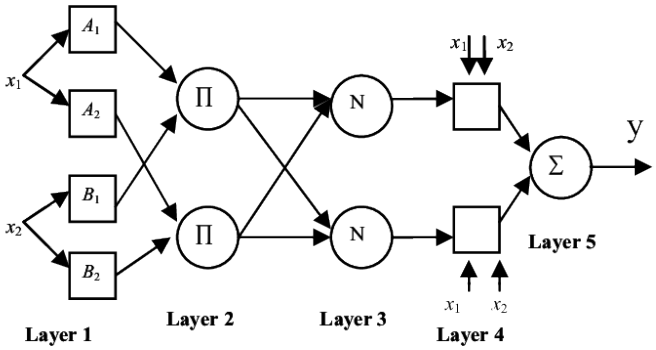

FIGURE 3. ANFIS architecture with input features [20].

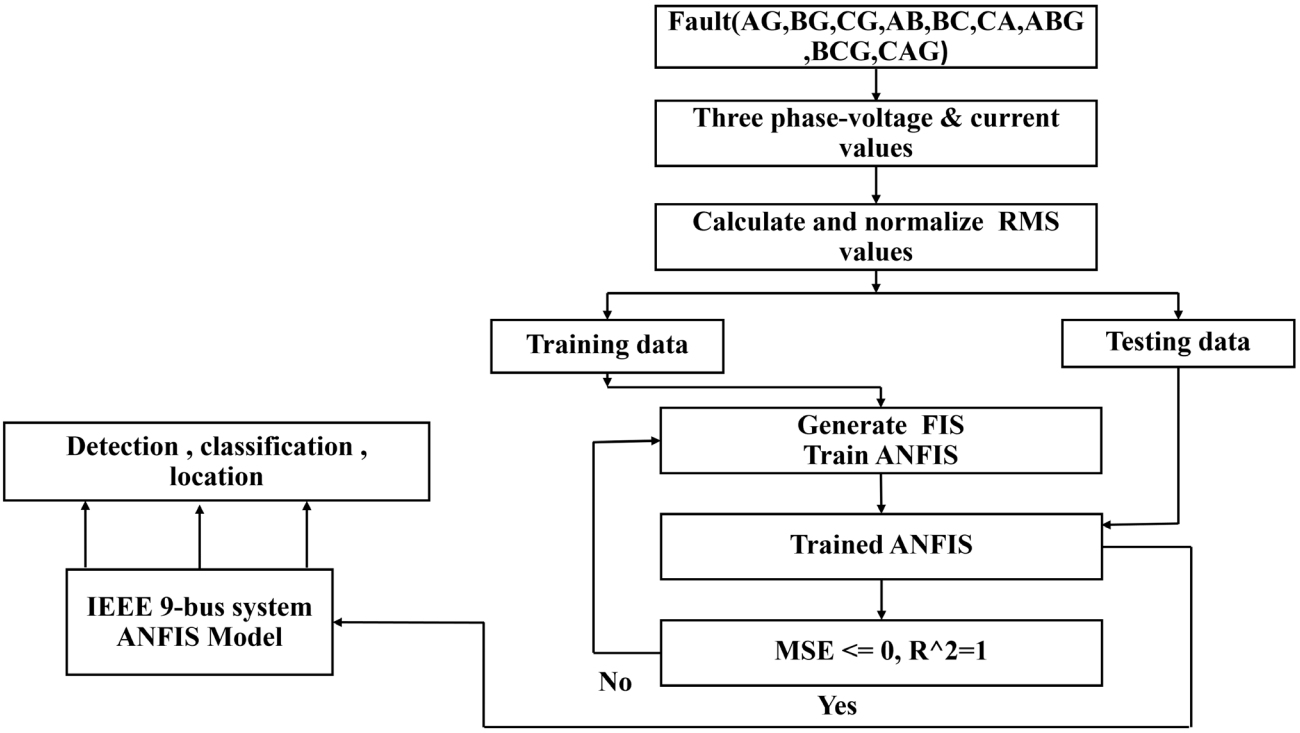

FIGURE 4. Flow chart for ANFIS-based fault model.

The flow diagram for ANFIS techniques is shown in Fig.4. The steps followed for the ANFIS model are as follows [30],[31]:
Step 1. Select the area in the power system for study; in this study, the area between bus seven and bus eight has been selected as shown in Fig. 1.
Step 2. Generate fault between bus seven and bus 8, and capture the voltage and current values from one end.
Step 3. Apply all fault conditions, AG, BG, CG, AB, BC, CA, ABG, BCG, CAG and no-fault

Step 4. Change the fault position and collect the faulty signal's voltage and current (rms)values.
Step 5. Normalization of the data
Step 6. Select the structure of ANFIS
Step 7. Choose input and target data
Step 8. Train ANFIS with the dataset
Step 9. Test the models
Step 10. Compute and record the percentage error and the Mean square error for the ANFIS-based detector, classifier, and location to check the performance of the ANFIS model.

2) BACK PROPAGATION NEURAL NETWORK (BPNN)

The ability of ANNs to work with complex systems makes ANNS a good network for fault detection, classification, and location [26].

Some of the properties that make ANNs better to work for complex and nonlinear tasks are as follows:

a) Every electrical system fault causes a change in the power system, and a neural network (NN) can reorganize according to these changes
b) ANN can make decisions and learn through experience
c) Due to their numerical strength, they can carry out several tasks at once.

The ANN offers a lot of benefits, but it also has certain drawbacks. The choice of network type, the number of hidden layers, the number of neurons, and the settings of the learning method are some crucial elements [4]. There are several limitations, such as post-fault values of line currents and voltages for fault identification and classification. The line current and voltage of the fault transmission lines are considerably different before and after the incident. Therefore, determining the type of faults from pre- and post-fault value patterns is necessary for the fault classification procedure. The BPNN basic structure and the network used in this paper are given in Fig. 5a and 5b, respectively. Correct weight tuning in BPNN reduces the error rate [32]. Weights are selected at random. The consequences are updated after each iteration or epoch, and the procedure is repeated. The following are some of BPNNs' most valuable benefits: Backpropagation may function without having thorough network expertise since it is simple, quick, and straightforward to implement [34],[7]. As shown in Fig. 5c the simple flow diagram of ANN-based fault detection. It just requires tuning a small number of input parameters, such as the number of hidden layers and neurons in each hidden layer. Levenberg-Marquardt backpropagation is used to modify the weights and biases of the training process. Additionally, the mean absolute error (MAE), root mean square error (RMSE), and mean square error (MSE) can be used to calculate learning errors.

The following equation 7 is used to compute RMSE, which has been used in this paper for the performance of the models.

$$RMSE = \sqrt{\sum_{i=1}^{n} \left(y_{predicted} - y_{actual}\right)^2} \quad (7)$$

This way, it generates the error for fault detection, classification, and location against the fault generated in the IEEE 9 system for each case of fault. The final output of BPNN generated for sample j can be calculated as below:

$$y_j = \sum_{j=1}^{n} \omega_{k,j} f(h_k) + \beta_j \quad (8)$$

The $\omega_{k,j}$ in equation 8 is the weight of hidden node k at the jth epoch. β_j is the bias value of the output node at the jth age. $f(h_k)$ is the output value of hidden node k. The fitness of values can be calculated using the Error in the equation below.

$$Fitness(x) = minimum(RMSE) \quad (9)$$

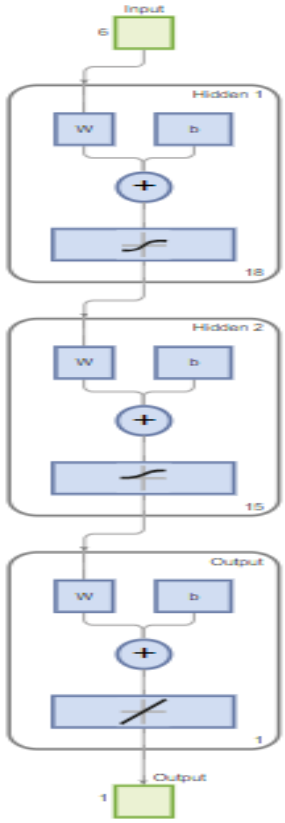

FIGURE 5b. ANN structure for Fault detection [21].

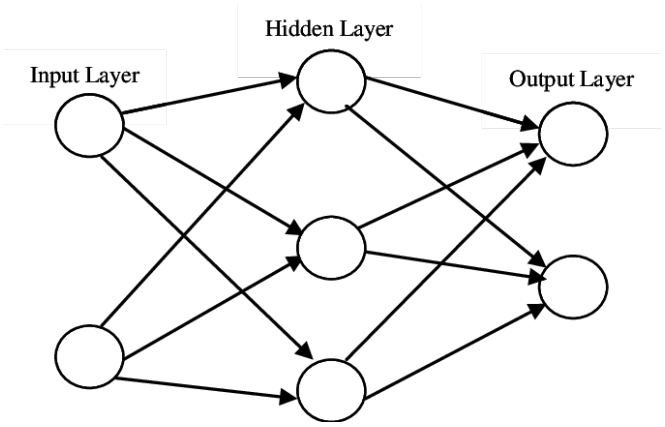

FIGURE 5a. BPNN basic structure [7].

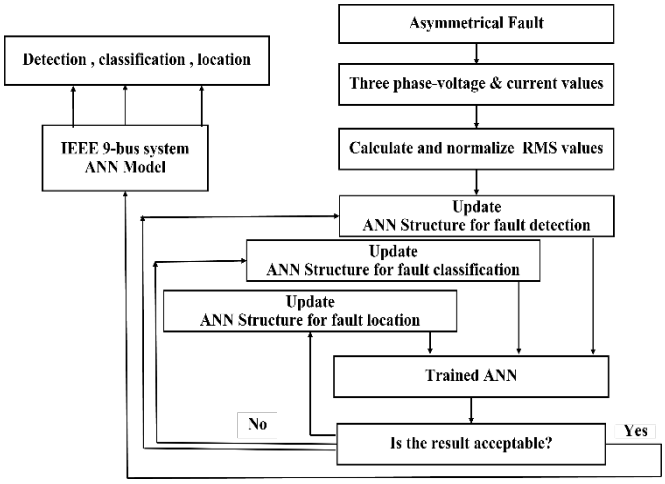

FIGURE 5c. Flow chart for ANN-based fault model.

3) SELF ORGANIZING MAP (SOM) NEURAL NETWORK

SOM is an extensively used neural model in the competitive learning network category. It uses unsupervised learning. Therefore, there is no need for human assistance during training or extensive prior knowledge of the input and output data. SOM is used for tasks like clustering input data and locating the faults.

The self-organizing map (SOM), which has strong visualization capabilities, is particularly well suited for data categorization tasks [27]. It produces a collection of prototype vectors to represent the data set. It projects the prototypes from the high-dimensional input space onto a low-dimensional grid while maintaining their structure. This ordered grid may be a practical visualization surface to display various SOM properties, such as the cluster structure. The structure is shown in Fig. 6a [22].

The voltage and current data set is first clustered using the Kohonen-mean clustering method. The k-means clustering technique divides a given data set into a predetermined number (k) of clusters.

The centroid's k number is initially picked. A data point at the cluster's center is called the centroid.

For this work, a two-dimensional SOM is used. A 2D lattice of 'nodes', each completely linked to the input layer, makes up the network. A Kohonen network of 8* 8 nodes connected to the input layer and representing a two-dimensional vector can be seen in Fig. 6a. Each node in the lattice has a distinct topological location and a vector of weights that has the same dimension as the input vectors. Afterward, a matching weight vector W with n dimensions is mapped with clustered input, as shown in Fig. 6a.

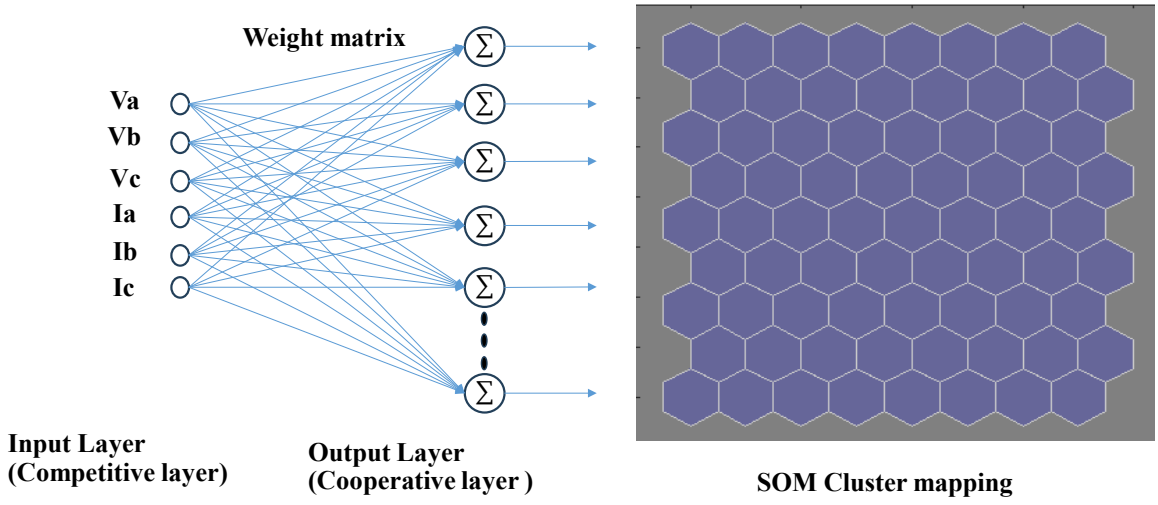

FIGURE 6a. SOM structure with clustered input.

Unlike many other types of networks, a SOM does not need a specific target output. Instead, the area of the lattice where the node weights match the input vector is specifically tuned to resemble the data for the class the input vector belongs to more closely. The SOM finally settles into a map of stable zones after starting with a distribution of random weights and going through several iterations. Training of SOM takes several steps [28],[33], which are mentioned below.

Step 1. Weight initialization

Step 2. Best matching unit (BMU) calculation using Euclidean distance method.

The Euclidean distance can be calculated using the following:

$$Distance = \sqrt{\sum_{i=0}^{i=n}(X_i - W_i)^2} \quad (10)$$

In equation (10), W_i is the input vector, and W_i is the weight vector of nodes.

Step 3. Calculating the size of BMU

$$\sigma(n) = \sigma_0 \exp\left(-\frac{n}{T}\right) \quad (11)$$

In equation 11, $\sigma(n)$ is the width of the lettuce the at time zero, n is the epoch, and T is the time constant

Step 4. Weights adjustment can be done using equation (12) and (13)

$$W_{new} = W_{old} + \mathrm{L}\,(\mathrm{X} - W_{old}) \quad (12)$$

$$W(n+1) = W(n) + L(n)\big(X(n) - W(n)\big) \quad (13)$$

In equations (12) and (13), L is the learning rate, W_{new} new weights, W_{old} is old weights, and X is the input vector.

The learning rate is calculated at each epoch using equation (14).

$$L(n) = L_0\, exp\left(-\frac{n}{T}\right) \quad (14)$$

In this paper, we preprocessed the data: six features of three-phase voltage and current. Meanwhile, the SOM parameters, such as grid size and number of input features for fault detection, classification, and location, are defined using the Matlab tool first, and changes are made in the SOM code according to the learning rate. The size of the grid as we test the grid for larger size; the higher the size, the better. We tested for as high as a 60*60 grid. After defining the features, we train the SOM model for detection, classification, and Location. After training, the training data and testing points to the SOM grid using the SOM function in Matlab [21].

Then, the fault type, fault detected value, and fault location within each mapped neuron were retrieved for training data. The flow diagram of the whole process is given in Fig. 6b. The weights generated by the SOM model for each input is given in Fig. 8a and Fig. 8b shows the distance created between all the neighboring weights.

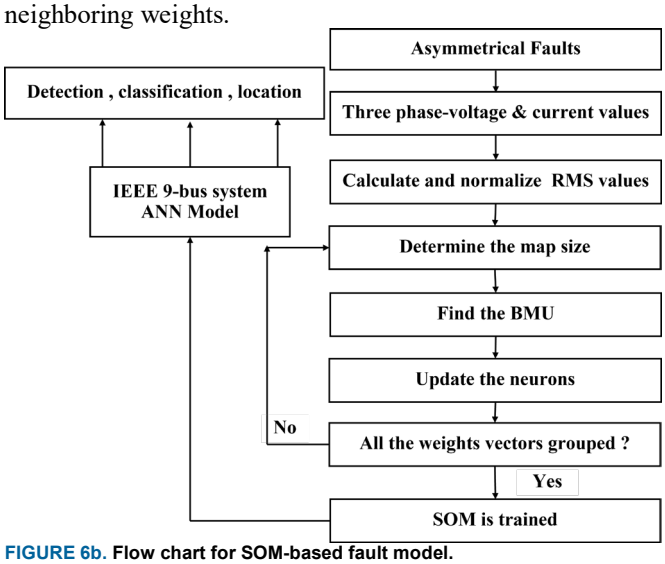

FIGURE 6b. Flow chart for SOM-based fault model.

4) DISCRETE WAVELET TRANSFORM AND ANFIS

Wavelet transform, using information from the frequency domain and time domain, can detect and classify different kinds of faults. Wavelet transform is sensitive to signal abnormalities [23]. In this algorithm, the DWT is employed to extract the detailed features of the current signal using the mother wavelet "db1". Several kinds of mother wavelets may be used to extract characteristics from the current signal. After several calculations using several wavelet families, it was determined that the Daubechies family's "db1" wavelet can accurately identify fault in the current signal [24]. The original current signals are divided into several frequency levels using wavelet algorithms. The mother wavelet is scaled and shifted throughout the signal to achieve this. DWT is used because the data being analyzed is digital [25].

The steps used to apply DWT are as follows.

Step 1. Record the current signal at bus number 7 in the IEEE 9-bus system.

Step 2. Apply DWT using the below equation [29],[35].

$$D = \frac{1}{\sqrt{2p}}\int_{-\infty}^{\infty} x(t)\varphi^*\left(\frac{t - q2p}{2p}\right)dt \quad (15)$$

Where p and q are the wavelet's scale and the wavelet function's positions. x(t) represents the current signal recorded at bus 7. φ^* is the complex conjugate and the mother wavelet.

Step 3. Decompose the current signal into high-frequency components and low-frequency components.

Step 4. Recording detailed components and approximate components to use it with ANFIS. It can be represented mathematically as.

$$a(t) = \sum_q x(t).h_q(2t - q) \quad (16)$$

$$d(t) = \sum_q x(t).g_q(2t - q) \quad (17)$$

Where a(t) is the approximate coefficient of the current signal extracted using the low pass filter (h_q), and d(t) is the detail coefficient of the current signal extracted using the high pass filter g_q.

Step 5. Use an Approximate and detailed coefficient and apply ANFIS by following the steps in ANFIS. After the training and testing, record the results to check the model's performance. As shown in the flow diagram in Fig. 7.

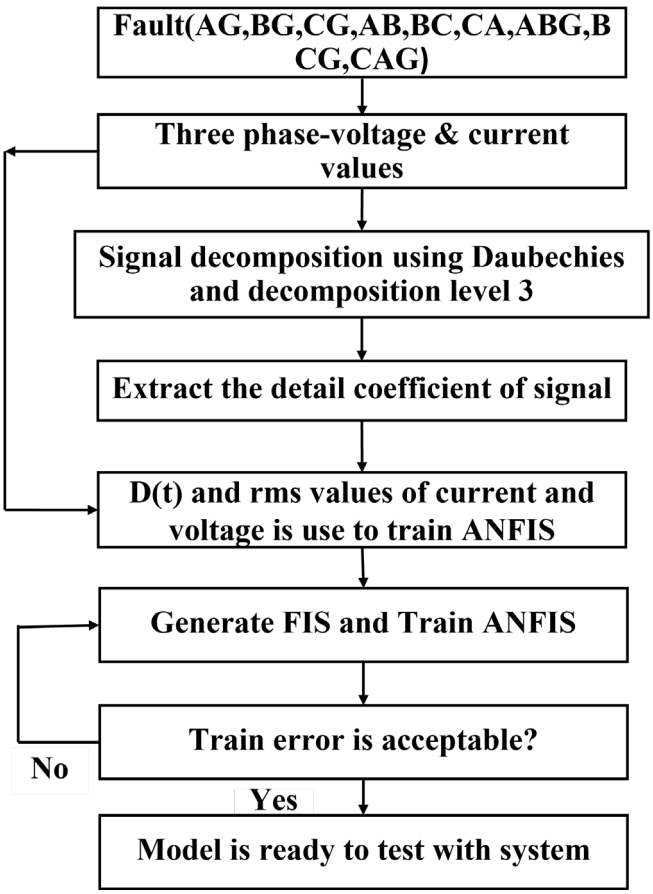

FIGURE 7. Flow chart for DWT-ANFIS-based fault model.

C. TRAINING AND TESTING

1) TRAINING TESTING DATA

For developing neural network-based models, arranging input and targets for a particular task is necessary. The two basic processes in a Neural network are training and testing with the input and target data to make predictions for upcoming events, in our case, predictions about fault detection, fault classification, and fault location. Training and testing input and out-sample data is mentioned in Table I.

For ANFIS, ANN, SOM, and DWT-ANFIS-based models, data is collected from bus number 7 in the IEEE 9-bus system after generating eight different types of faults and for no-fault conditions. The eight fault cases are A-G, B-G, C-G, AB, BC, CA, AB-G, BC-G, CA-G faults. All these faults are generated at four locations at the transmission line between bus number 7 and bus number 8 in the IEEE 9-bus model simulated in MATLAB/Simulink [21]. Training and testing data, in the form of root mean square values of three-phase current and three-phase voltage, are collected and preprocessed for the next step. 80% of the total data is used as training data, and 20% is used as testing data. For the development of ANFIS-based fault detection, classification, and Location models, a Fuzzy C-mean (FCM) Clustering algorithm is used. The total clusters used are 50, and the total membership for each cluster is 50, too. The Gaussian input membership function is further used as a membership function for inputs.

After generating a trained ANFIS network for fault detection, classification, and Location, the trained network is saved and used with the simulated model to get the results. The generated ANFIS Network is presented in Fig.10.

An ANN-based fault model for detection, classification, and location, a MATLAB toolbox, is used. The generated MATLAB code is further used. To adjust the parameters to make the model better. 80% of the data is used for training, and 20% is used for testing and validation. Two hidden layers are used, and the hidden neurons in each layer are 18 and 15, respectively, with sigmoid and tan sigmoid membership functions.

The workflow for the developed ANFIS model is given in Fig. 4.

For SOM, the train data is the root mean squared value of three-phase voltage and current. The dimension defined for the SOM for detection is 8*8. The clusters generated are mapped with the target to evaluate the performance. The clustered mapping is shown in Fig. 6a.

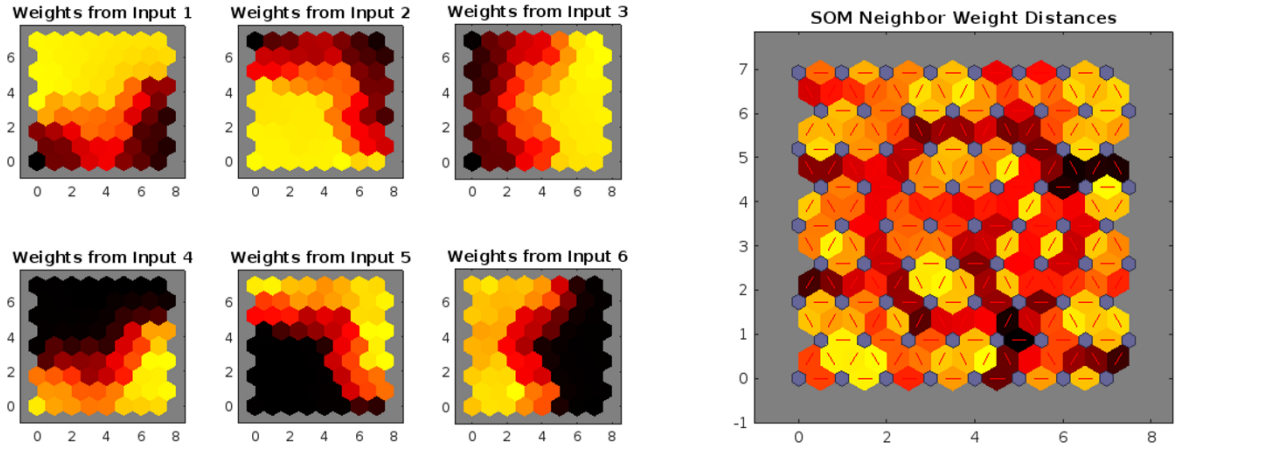

a) **b)**

FIGURE 8 a). Weights for each input, b) Neighbor distance between weights.

TABLE I
SAMPLE DATA SET FOR THE ANFIS-BASED FAULT DETECTION, CLASSIFICATION, AND FOR LOCATION

	Input data						Output data		
Fault case	**Va**	**Vb**	**Vc**	**Ia**	**Ib**	**Ic**	**Detection**	**classification**	**Location**
AG	0.1311	0.6292	0.6068	2.1012	0.3729	0.3622	1	1	25,50,75,100
BG	0.606	0.1213	0.6297	0.3651	2.0097	0.3712	1	2	25,50,75,100
CG	0.63	0.6069	0.1616	0.3717	0.3642	1.5324	1	3	25,50,75,100
AB	0.2912	0.3291	0.6116	2.305	2.0751	0.3619	1	4	25,50,75,100
BC	0.6116	0.2981	0.3451	0.3619	1.7722	1.4873	1	5	25,50,75,100
CA	0.3487	0.6116	0.2997	1.4149	0.3619	1.7019	1	6	25,50,75,100
ABG	0.1178	0.1282	0.6235	2.1606	2.176	0.3723	1	7	25,50,75,100
BCG	0.6235	0.1087	0.1312	0.3709	2.0516	1.6206	1	8	25,50,75,100
CAG	0.1459	0.6237	0.1367	2.0298	0.3716	1.5825	1	9	25,50,75,100
No fault	0.611627	0611627	0.611627	0.361749	0.361749	0.361749	0	0	25,50,75,100

2) FAULT DETECTION

The ANFIS-based fault detection model detects the fault while analyzing the three-phase voltage and current signal. The RMS value of three-phase voltage and post-fault current are inputs for the fault detection model. The output of the fault detection model is two binary states: 1 or 0. The one indicates a fault, and 0 shows a no-fault condition. The fault detection modal structure in MATLAB for ANN and ANFIS is given in Fig. 5b and Fig.10.

Fault detection takes six inputs (three-phase voltage and three-phase current) and one output to display whether there is a fault or no fault in the system.

The same input and output datasets are used for ANN and SOM for training and testing, and trained models are used with the system for fault detection. For the fault detection model of DWT-ANFIS, the detail coefficient of the faulty current signal is used in addition to the raw voltage and current signal values for training and testing of the DWT-ANFIS model.

3) FAULT CLASSIFICATION

The ANFIS-based fault classification model is designed and trained for the same input as the fault detection model. The output for fault classification is changed; for fault classification, we used one output indicating the fault class. Table I shows that the fault class output is eight numerical values for eight different fault classes and 0 for no-fault conditions.

The ANFIS-based fault classification structure is given in Fig. 7. The total input for the fault classification model is 6, and the output is 1. When the trained model is tested with the system post-fault rms values of three-phase voltage and current, the model gives the output based on the fault generated. According to the results shown in Table I, the system has the respective fault.

The same inputs and outputs are employed by ANN and SOM-based classification models for training and testing. For the fault classification model of DWT-ANFIS, the detail coefficient of the faulty current signal is used in addition to the raw voltage and current signal values for training and testing of the DWT-ANFIS model. The performance of all models is simulated and recorded in Tables VI and VII for all the models.

4) FAULT LOCATION

ANFIS fault location trained model is developed for six inputs and one output for four different locations. The Location is in kilometers (km), and the eight various faults are generated at 100km, 75km, 50km, and 25km. The model is trained with the generated data for 40 different fault conditions.

The trained model is then tested with different conditions and three-phase current and voltage values; the results are given in the next section.

The same inputs and outputs as in ANFIS are used with ANN and SOM models for training and testing to find the Location of the fault generated in the system. For the Fault detection model of DWT-ANFIS, the detail coefficient of the faulty current signal is used in addition to the raw voltage and current signal values for training and testing of the DWT-ANFIS

model. The results for all the models are displayed in the results section in Tables VI and VII.

The first six columns in the Table are six inputs, and the last three columns are output data.

III. RESULT AND COMPARISON OF MODELS

A total number of 40 different fault conditions have been studied. Ten fault types are generated in the IEEE-9 bus system at four locations. Nine asymmetrical faults and no-fault states to analyze the performance of the proposed technique. These faults were caused on transmission lines at four different locations at different times.

The ANFIS model is trained and tested for six inputs and one output for fault detection. The results from the training and testing of ANFIS are given in Table II. Predicted fault detection, classification, and Location have been recorded, and percentage error has been computed for each case. The average percentage error for ANFIS-based fault detection, type, and Location is 0.008%. -0.005% and 0.547%, respectively. Which is less than zero. Compared to other models, the based model can detect all faults accurately, as shown in Table II, it detected all faults correctly. For Fault classification, the ANFIS model classified all fault classes with less than zero percent error. However, for the AB-G fault, the percentage error is -1.224 at 100 km. For fault location, ANFIS performed well with an average percent error of 0.547%. The root mean square error and mean absolute error are calculated and recorded in Table VII.

ANN-based models are given in Table III. The average percentage error is recorded in Table VI. The average percentage error for ANN-based Fault detection, classification, and Location is zero, 0.268, and 0.348 percent. The root mean square error. It can detect the fault correctly with zero percent error and classify the error with less than zero percent error except for phase C to A fault at 25km and phase A to phase B fault at 50 km.

Fault detection in the SOM-based model is computed in Table IV. The SOM clustered accurately for fault detection for all the faults and did not miss any fault with zero percentage error. In the case of SOM-based fault classification, the percentage error for all classifications is zero. However, the percentage error is more than one percent for AB-G fault classification at 100 km, as shown in Table. IV. Fault location is predicted well for most fault locations with zero percent error; however, it cannot detect the Location for two fault conditions at 100km and once for 50km, as shown in Table IV. The weight plane representation of the SOM classes displaying each of the six input features is shown in Fig. 8 (a), providing a visual depiction of the weights that link each input to a single neuron in the 6*8 hexagonal grid. Heavy weights are indicated by darker hues than lighter ones. Six inputs are highly correlated when they have comparable weight planes (color gradients can be inverted or identical). It was also shown that the weight ratios of voltage and current are opposite to one another when all four variables are weighted equally. Consequently, the Euclidean interval between each neuron's class and its surroundings is shown in Fig. 8(b). The input space's highly related regions are indicated by the vivid connections. On the other hand, groups representing areas of the function space that have few or no members separating them are shown by the dark links. Large swaths of the input space are divided by extended boundaries with dark connections, indicating that the groups on either side of the boundary reflect substantially different neighborhoods.

The DWT-ANFIS-based fault model predicted results are computed and recorded in Table V. The percentage error for fault detection for all the fault conditions is zero, as shown in Table V. Performance of DWT-ANFIS based model needs more improvement as the average percentage error for fault classification is -0.364% as shown in Table VI. For fault location, the DWT-ANFIS-based model detected fault location with a percentage error less than zero for most cases. Still, for some, the percentage error is 1 percent, as shown in Table V. The average error for this model is recorded in Table VI.

The average percentage error for all the models is computed and recorded in Table VI.

TABLE II
PERFORMANCE OF ANFIS -BASED FAULT DETECTION, CLASSIFICATION AND LOCATION MODEL

Fault type	Actual Location (km)	ANFIS predicted fault detection	% error in the ANFIS model	ANFIS estimated classification	% error in the ANFIS model	ANFIS predicted fault Location(km)	% error in the ANFIS model
1 (A-G)	**25**	1.000	0.048	1.000	-0.008	25.321	1.282
2 (B-G)	**25**	1.000	-0.005	2.000	-0.001	23.393	-6.427
3 (C-G)	**25**	1.001	0.062	3.002	0.065	24.798	-0.806
4 (AB)	**25**	1.000	0.001	4.000	0.002	25.007	0.029
5 (BC)	**25**	1.000	0.000	5.000	0.004	24.614	-1.545
6 (CA)	**25**	1.000	-0.015	5.999	-0.016	25.062	0.248
7(AB-G)	**25**	1.000	0.000	7.000	0.000	24.995	-0.020
8(BC-G)	**25**	1.000	0.007	8.000	0.002	24.994	-0.026
9(CA-G)	**25**	1.000	0.000	9.000	-0.003	24.853	-0.588
1 (A-G)	**50**	1.000	-0.004	1.000	0.000	49.967	-0.067
2 (B-G)	**50**	1.000	0.002	2.000	-0.005	48.434	-3.131
3 (C-G)	**50**	1.000	-0.001	3.000	-0.008	50.326	0.653
4 (AB)	**50**	1.000	0.000	4.000	0.000	50.231	0.462
5 (BC)	**50**	1.000	0.002	5.000	0.008	49.777	-0.447
6 (CA)	**50**	1.000	-0.001	6.000	-0.002	49.615	-0.769
7(AB-G)	**50**	1.000	0.003	7.000	0.000	50.214	0.428
8(BC-G)	**50**	1.000	0.004	8.000	-0.003	49.769	-0.463
9(CA-G)	**50**	1.000	-0.004	9.000	-0.005	50.526	1.052
1 (A-G)	**75**	1.000	0.009	1.000	0.014	73.761	-1.653
2 (B-G)	**75**	1.000	-0.001	2.000	-0.001	74.374	-0.835
3 (C-G)	**75**	1.000	-0.002	3.000	-0.006	74.837	-0.217
4 (AB)	**75**	1.003	0.347	4.025	0.624	74.599	-0.535
5 (BC)	**75**	1.000	0.000	4.999	-0.010	75.542	0.722
6 (CA)	**75**	1.000	-0.002	6.000	-0.001	75.935	1.246
7(AB-G)	**75**	1.000	0.000	7.000	0.001	75.354	0.472
8(BC-G)	**75**	1.000	-0.003	8.000	0.006	75.195	0.260
9(CA-G)	**75**	1.000	-0.005	9.000	-0.005	75.290	0.387
1 (A-G)	**100**	1.000	-0.008	1.000	-0.002	99.467	-0.533
2 (B-G)	**100**	1.000	-0.005	2.000	0.003	99.083	-0.917
3 (C-G)	**100**	1.000	-0.007	3.000	0.002	99.956	-0.044
4 (AB)	**100**	1.000	0.025	3.999	-0.023	99.237	-0.763
5 (BC)	**100**	1.000	0.000	5.000	0.007	100.910	0.910
6 (CA)	**100**	1.000	-0.049	6.002	0.033	99.000	-1.000
7(AB-G)	**100**	0.999	-0.066	6.914	-1.224	96.193	-3.807
8(BC-G)	**100**	1.000	-0.004	8.002	0.028	99.098	-0.902
9(CA-G)	**100**	1.000	-0.047	9.030	0.331	97.667	-2.333

TABLE III
PERFORMANCE OF ANN BASED FAULT DETECTION, CLASSIFICATION AND LOCATION MODEL

Fault type	Actual Location (km)	ANN predicted fault detection	%error in the ANN model	ANN predicted fault classification	%error in the ANN model	ANN predicted fault location (km)	%error in the ANN model
1 (A-G)	**25**	1.000	0.000	1.003	0.262	25.728	2.911
2 (B-G)	**25**	1.000	0.000	2.004	0.209	25.076	0.303
3 (C-G)	**25**	1.000	0.000	2.990	-0.320	25.974	3.898
4 (AB)	**25**	1.000	0.000	3.999	-0.034	26.860	7.441
5 (BC)	**25**	1.000	0.001	4.996	-0.071	23.738	-5.048
6 (CA)	**25**	1.000	0.000	5.315	-11.414	26.235	4.941
7(AB-G)	**25**	1.000	0.000	6.995	-0.066	24.736	-1.057
8(BC-G)	**25**	1.000	0.001	8.002	0.024	25.141	0.564
9(CA-G)	**25**	1.000	0.000	9.000	0.005	25.457	1.828
1 (A-G)	**50**	1.000	0.000	1.006	0.592	49.565	-0.871
2 (B-G)	**50**	1.000	0.000	2.001	0.038	48.177	-3.646
3 (C-G)	**50**	1.000	0.000	2.994	-0.185	49.645	-0.710
4 (AB)	**50**	1.000	0.000	4.220	5.491	50.485	0.970
5 (BC)	**50**	1.000	-0.001	5.002	0.040	49.147	-1.705
6 (CA)	**50**	1.000	0.000	6.008	0.140	46.300	-7.400
7(AB-G)	**50**	1.000	0.000	6.999	-0.009	50.638	1.276
8(BC-G)	**50**	1.000	0.000	8.001	0.016	49.403	-1.194
9(CA-G)	**50**	1.000	0.000	9.000	-0.002	50.350	0.700
1 (A-G)	**75**	1.000	0.000	1.003	0.280	76.945	2.594
2 (B-G)	**75**	1.000	0.000	1.999	-0.052	74.808	-0.256
3 (C-G)	**75**	1.000	0.000	2.996	-0.136	74.277	-0.964
4 (AB)	**75**	1.000	0.007	3.875	-3.124	79.080	5.440
5 (BC)	**75**	1.000	0.000	5.002	0.048	77.279	3.039
6 (CA)	**75**	1.000	0.000	5.993	-0.117	76.491	1.987
7(AB-G)	**75**	1.000	0.000	6.998	-0.033	76.164	1.552
8(BC-G)	**75**	1.000	0.000	8.005	0.061	74.680	-0.427
9(CA-G)	**75**	1.000	0.000	8.992	-0.092	75.423	0.564
1 (A-G)	**100**	1.000	-0.001	0.997	-0.350	98.511	-1.489
2 (B-G)	**100**	1.000	-0.001	2.008	0.412	98.845	-1.155
3 (C-G)	**100**	1.000	0.001	2.994	-0.196	99.044	-0.956
4 (AB)	**100**	1.000	0.000	3.973	-0.666	99.556	-0.444
5 (BC)	**100**	1.000	0.000	5.005	0.106	99.152	-0.848
6 (CA)	**100**	1.000	0.003	6.028	-0.468	99.860	-0.140
7(AB-G)	**100**	1.000	0.000	6.997	-0.037	101.668	1.668
8(BC-G)	**100**	1.000	0.000	7.995	-0.063	100.301	0.301
9(CA-G)	**100**	1.000	-0.001	9.006	0.064	100.165	0.165

TABLE IV
PERFORMANCE OF SOM -BASED FAULT DETECTION, CLASSIFICATION AND LOCATION MODEL

Fault type	Actual Location (km)	SOM predicted fault detection	%error in the SOM model	SOM predicted fault classification	%error in the SOM model	SOM predicted fault location (km)	%error in the SOM model
1 (A-G)	**25**	1.000	0.000	1	0.000	25	0
2 (B-G)	**25**	1.000	0.000	2	0.000	25	0
3 (C-G)	**25**	1.000	0.000	3	0.000	25	0
4 (AB)	**25**	1.000	0.000	4	0.000	25	0
5 (BC)	**25**	1.000	0.000	5	0.000	25	0
6 (CA)	**25**	1.000	0.000	6	0.000	25	0
7 (AB-G)	**25**	1.000	0.000	7	0.000	25	0
8 (BC-G)	**25**	1.000	0.000	8	0.000	25	0
9 (CA-G)	**25**	1.000	0.000	9	0.000	25	0
1 (A-G)	**50**	1.000	0.000	1	0.000	50.000	0
2 (B-G)	**50**	1.000	0.000	2	0.000	50.000	0
3 (C-G)	**50**	1.000	0.000	3	0.000	50.000	0
4 (AB)	**50**	1.000	0.000	4	0.000	43.750	-12.5
5 (BC)	**50**	1.000	0.000	5	0.000	50.000	0
6 (CA)	**50**	1.000	0.000	6	0.000	50.000	0
7 (AB-G)	**50**	1.000	0.000	7	0.000	50.000	0
8 (BC-G)	**50**	1.000	0.000	8	0.000	50.000	0
9 (CA-G)	**50**	1.000	0.000	9	0.000	50.000	0
1 (A-G)	**75**	1.000	0.000	1	0.000	75.000	0
2 (B-G)	**75**	1.000	0.000	2	0.000	75.000	0
3 (C-G)	**75**	1.000	0.000	3	0.000	75.000	0
4 (AB)	**75**	1.000	0.000	4	0.000	75.000	0
5 (BC)	**75**	1.000	0.000	5	0.000	75.000	0
6 (CA)	**75**	1.000	0.000	6	0.000	75.000	0
7 (AB-G)	**75**	1.000	0.000	7	0.000	75.000	0
8 (BC-G)	**75**	1.000	0.000	8	0.000	75.000	0
9 (CA-G)	**75**	1.000	0.000	9	0.000	75.000	0
1 (A-G)	**100**	1.000	0.000	1	0.000	97.22222	-2.77778
2 (B-G)	**100**	1.000	0.000	2	0.000	100	0
3 (C-G)	**100**	1.000	0.000	3	0.000	100	0
4 (AB)	**100**	1.000	0.000	4	0.000	100	0
5 (BC)	**100**	1.000	0.000	5	0.000	100	0
6 (CA)	**100**	1.000	0.000	6	0.000	97.91667	-2.08333
7 (AB-G)	**100**	1.000	0.000	6.727273	-3.896	100	0
8 (BC-G)	**100**	1.000	0.000	8	0.000	100	0
9 (CA-G)	**100**	1.000	0.000	9	0.000	100	0

TABLE V
PERFORMANCE OF DWT-ANFIS-BASED FAULT DETECTION, CLASSIFICATION, AND LOCATION MODEL

Fault type	Actual Location (km)	DWT-ANFIS predicted fault detection	% error in DWT-ANFIS model	DWT-ANFIS estimated classification	% error in DWT-ANFIS model	DWT-ANFIS predicted fault Location(km)	% error in DWT-ANFIS model
1 (A-G)	**25**	1.000	0.000	0.998938	-0.106	24.98329	-0.06685
2 (B-G)	**25**	1.000	-0.002	1.99655	-0.172	25.339	1.35648
3 (C-G)	**25**	1.000	0.002	2.9338	-2.207	25.124	0.42975
4 (AB)	**25**	1.000	0.000	3.98245	-0.439	24.832	-0.67328
5 (BC)	**25**	1.000	0.000	4.743457	-5.131	25.393	1.572514
6 (CA)	**25**	1.000	0.000	6.036992	0.617	25.079	0.314833
7 (AB-G)	**25**	1.000	0.000	7.015356	0.219	25.036	0.142133
8 (BC-G)	**25**	1.000	0.001	7.896957	-1.288	25.145	0.578229
9 (CA-G)	**25**	1.000	0.000	8.9781	-0.243	25.001	0.005714
1 (A-G)	**50**	1.000	-0.004	1.0003	0.030	49.739	-0.52184
2 (B-G)	**50**	1.000	-0.003	2.0022	0.110	50.149	0.297455
3 (C-G)	**50**	1.000	0.001	2.99994	-0.002	49.991	-0.01704
4 (AB)	**50**	1.000	0.002	4.000488	0.012	50.098	0.19635
5 (BC)	**50**	1.000	0.000	5.00839	0.168	49.846	-0.30706
6 (CA)	**50**	1.000	-0.002	6.0378	0.630	49.822	-0.35572
7 (AB-G)	**50**	1.000	0.000	7.002743	0.039	49.940	-0.12011
8 (BC-G)	**50**	1.000	0.000	8.014625	0.183	49.982	-0.03545
9 (CA-G)	**50**	1.000	-0.002	9.01562	0.174	50.000	-0.0004
1 (A-G)	**75**	1.000	-0.003	0.982418	-1.758	74.959	-0.05485
2 (B-G)	**75**	1.000	0.000	1.999891	-0.005	75.054	0.071576
3 (C-G)	**75**	1.000	0.000	2.999	-0.033	75.051	0.068133
4 (AB)	**75**	1.000	0.002	4.00061	0.015	75.202	0.26868
5 (BC)	**75**	1.000	0.001		0.181	75.198	0.263827
6 (CA)	**75**	1.000	-0.001	5.99218	-0.130	74.826	-0.23177
7 (AB-G)	**75**	1.000	-0.001	6.998723	-0.018	75.233	0.310482
8 (BC-G)	**75**	1.000	0.002	7.936269	-0.797	75.020	0.026992
9 (CA-G)	**75**	1.000	-0.004	8.998229	-0.020	74.994	-0.0076
1 (A-G)	**100**	1.000	-0.001	1.002144	0.214	99.940	-0.06031
2 (B-G)	**100**	1.000	0.007	1.9999	-0.005	99.139	-0.86128
3 (C-G)	**100**	1.000	0.000	2.99182	-0.273	100.022	0.02181
4 (AB)	**100**	1.000	0.002	3.98418	-0.396	99.978	-0.02236
5 (BC)	**100**	1.000	0.000	5.016222	0.324	99.943	-0.05733
6 (CA)	**100**	1.000	0.001	6.0023	0.038	99.830	-0.17002
7 (AB-G)	**100**	1.000	0.001	6.867009	-1.900	99.703	-0.29667
8 (BC-G)	**100**	1.000	0.002	8.007442	0.093	99.926	-0.07367
9 (CA-G)	**100**	1.000	-0.001	8.89006	-1.222	100.025	0.0247

TABLE VI
PERCENTAGE ERROR COMPARISON OF ANN, ANFIS, WT-ANFIS, AND SOM MODELS

Task	ANFIS	ANN	SOM	DWT-ANFIS
Fault Detection (%)	0.008	0.000	0.000	0.000
Fault Classification (%)	-0.005	-0.268	-0.108	-0.364
Fault Location (%)	-0.547	0.384	-0.482	0.056
Average (%)	0.0015	0.039	-0.197	-0.103

The performance of various models including ANN, ANFIS, SOM, and DWT-ANFIS are illustrated in Fig. 9 a, b, and c, representing fault detection, classification, and location respectively. Fig. 9a showcases the fault detection capabilities of these models across forty distinct scenarios, each assessed with a testing dataset comprising 400 instances. The simulation was conducted for fault (1) and no-fault (0) conditions, with all models demonstrating accurate detection capabilities for both scenarios.

For fault classification, depicted in Fig. 9b, the models' performance is evaluated across ten fault classes (AG, BG, CG, AB, BC, CA, ABG, BCG, CAG) as well as the no-fault case. While overall performance was satisfactory, certain fault classes exhibited lower accuracy, particularly with ANN and DWT-ANFIS models.

In the context of fault location prediction, the models were tested across four distinct locations. ANFIS and SOM notably achieved precise location predictions, as depicted in Fig. 9c, outperforming the other models in this regard.

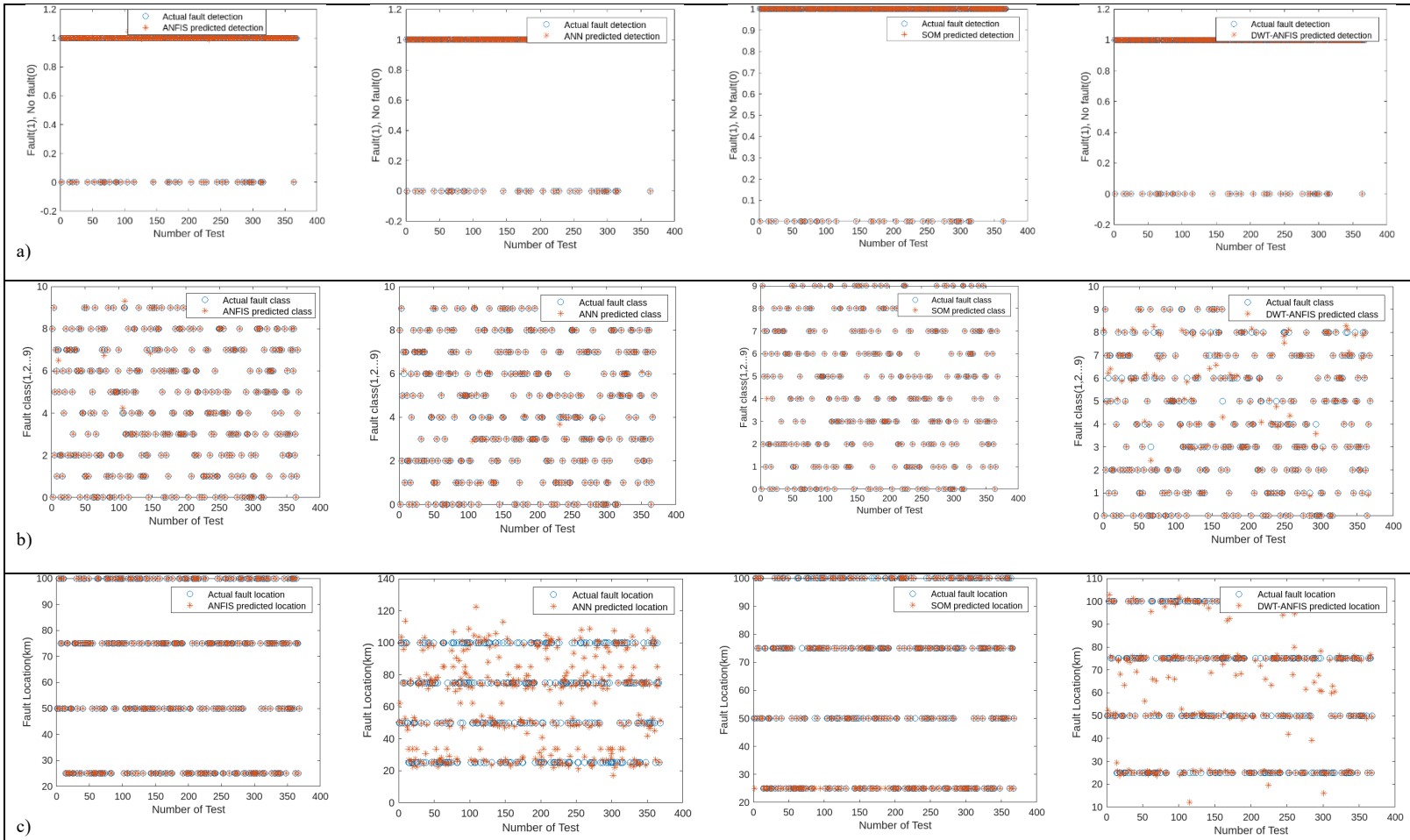

ANFIS-based fault detection, classification, and Location | ANN-based fault detection, classification, and Location | SOM-based fault detection, classification, and Location | DWT-ANFIS-based fault detection, classification, and Location

FIGURE 9. The performance of ANFIS, ANN, SOM, and DWT-ANFIS models for testing: a. Fault detection, b: fault classification, c: fault location

TABLE VII
TRAINING AND TESTING PERFORMANCE OF ANN, ANFIS, DWT-ANFIS AND SOM BASED MODELS

Models	Technique	Training				Testing			
		RMSE	MAE	R^2	Time(minute)	RMSE	MAE	R^2	Time(s)
Detection	ANN	0.000	0.000	1.000	13.00422	0.000	0.000	1.000	0.219179
	ANFIS	0.000	0.000	1.000	612.345	0.000	0.000	1.000	0.210096
	DWT-ANFIS	0.000	0.000	1.000	1235.60	0.000	0.000	1.000	0.205
	SOM	0.000	0.000	1.000	17.4816	0.000	0.000	1.000	0.0030
Classification	ANN	0.061	0.009	0.999	13.4822	0.062	0.014	0.999	0.099
	ANFIS	0.000	0.000	1.000	579.63	0.019	0.003	0.999	0.203
	DWT-ANFIS	0.003	0.000	1.000	1205.18	0.133	0.038	0.998	0.229
	SOM	0.000	0.000	1.000	8.206	0.1564	0.0082	0.997	0.001763
Location	ANN	4.229	2.664	0.977	19.069	5.171	3.271	0.966	0.0533
	ANFIS	1.118	0.664	0.999	1800.12	1.880	1.142	0.996	0.299
	DWT-ANFIS	7.199	2.191	0.933	1241.629	7.234	2.161	0.935	0.2016
	SOM	1.129	0.051	0.998	34.362	14.744	3.669	0.726	0.001173

The performance of models in the form of RMSE given in equation, mean absolute error, and R^2 is recorded in Table VII.

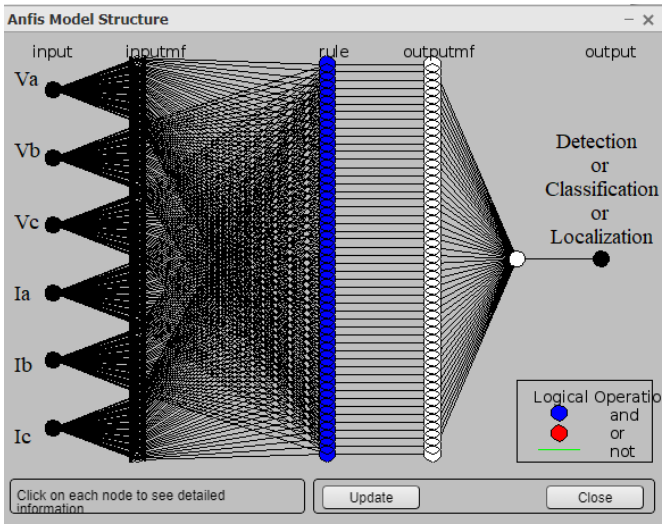

FIGURE 10. ANFIS network for fault models [21],[30].

$$\%Error = \left(\frac{Predicted\ value - Actual\ value}{Actual\ value}\right) * 100 \quad (18)$$

$$MAE = \sum_{i=1}^{n} \frac{|Predicted\ value - Actual\ value|}{n} \quad (19)$$

The output graph between predicted values and actual fault is given in Fig. 9a for ANFIS, ANN, SOM, and DWT-ANFIS models. Similarly, Fig. 9b shows the predicted value and actual classification for fault for all four models. Further, Fig. 9c represents the exact fault location and predicted Location for model ANFIS, ANN, SOM, and DWT-ANFIS.

V. CONCLUSION

In this study, we compared the effectiveness of several methods, including Artificial Neural Networks (ANN), Adaptive Neuro-Fuzzy Inference Systems (ANFIS), Self-Organizing Maps (SOM), and a hybrid approach that combines Discrete Wavelet Transform (DWT) with ANFIS, for fault

detection, classification, and localization in transmission lines. Our study set out to investigate the effectiveness of these techniques in managing the complex tasks (faults) that are a part of power transmission networks. Our findings show that the average percentage error for each of the approaches under investigation differs significantly. The average percentage error for the ANN-based models was 0.039, which is a good result. But with a noticeably lower average percentage error of 0.0015, the ANFIS-based models beat their ANN counterparts, demonstrating the greater adaptability and robustness of the ANFIS technique in fault identification.

The SOM-based models showed an average percentage error of -0.197, which can be explained by the special properties of SOMs and their effective mapping of high-dimensional data to low-dimensional space. This negative error number shows how well the SOM-based models handled complicated transmission line fault situations by continuously producing findings that were closer to ground truth values.

Additionally, with an average percentage error of -0.103, the hybrid strategy that combined DWT with ANFIS demonstrated a significant improvement. This enhancement highlights how well DWT and ANFIS operate together, using DWT's signal processing capabilities to improve the ANFIS framework's fault detection, classification, and location accuracy.

Overall, our comparative analysis demonstrates how well ANFIS and hybrid approaches work to address the problems related to fault localization, classification, and detection in transmission lines. These results highlight the need of utilizing cutting-edge computational methods and hybrid strategies to improve the dependability and effectiveness of electricity transmission networks.

ACKNOWLEDGEMENT

The authors would like to acknowledge the support of the Department of Electrical Engineering, School of Engineering, and authors would also like to thank the research fund (grant number KDS2021/021) from King Mongkut's Institute of Technology Ladkrabang (KMITL), Bangkok 10520, Thailand.

REFERENCES

[1] D. Lu, Y. Liu, Q. Liao, B. Wang, W. Huang and X. Xi, "Time-Domain Transmission Line Fault Location Method With Full Consideration of Distributed Parameters and Line Asymmetry," in *IEEE Transactions on Power Delivery*, vol. 35, no. 6, pp. 2651-2662, Dec. 2020, doi: 10.1109/TPWRD.2020.2974294.

[2] A. Yadav, and A. Swetapadma. "A single ended directional fault section identifier and fault locator for double circuit transmission lines using combined wavelet and ANN approach." *International Journal of Electrical Power & Energy Systems*, vol. 69, pp. 27-33, Jul. 2017, doi: 10.1016/j.ijepes.2014.12.079.

[3] Z. Jiao and R. Wu, "A New Method to Improve Fault Location Accuracy in Transmission Line Based on Fuzzy Multi-Sensor Data Fusion," in IEEE Transactions on Smart Grid, vol. 10, no. 4, pp. 4211-4220, July 2019, doi: 10.1109/TSG.2018.2853678.

[4] A. Abdullah, "Ultrafast Transmission Line Fault Detection Using a DWT-Based ANN," in IEEE Transactions on Industry Applications, vol. 54, no. 2, pp. 1182-1193, March-April 2018, doi: 10.1109/TIA.2017.2774202.

[5] M. T. Hoq, "Distance Protection of Transmission Lines with High Levels of Series Compensation: A study on frequency and time domain communication independent distance protection for series compensated lines." PhD diss., KTH Royal Institute of Technology, 2023.

[6] M. J. B. Reddy and D. K. Mohanta, "Performance Evaluation of an Adaptive-Network-Based Fuzzy Inference System Approach for Location of Faults on Transmission Lines Using Monte Carlo Simulation," in IEEE Transactions on Fuzzy Systems, vol. 16, no. 4, pp. 909-919, Aug. 2008, doi: 10.1109/TFUZZ.2008.924210.

[7] D. P. Mishra, and P. Ray. "Fault detection, location and classification of a transmission line." *Neural Computing and Applications*, vol. 30, pp. 1377-1424, Sep. 2018, doi: 10.1007/s00521-017-3295-y.

[8] E. E. Nagu, and K. Ramar. "A combined impedance and traveling wave based fault location method for multi-terminal transmission lines." *International Journal of Electrical Power & Energy Systems*, vol. 33, no. 10, pp. 1767-1775, Dec. 2011, doi: 10.1016/j.ijepes.2011.08.020.

[9] A. Mukherjee, P. K. Kundu, and A. Das. "Transmission line faults in power system and the different algorithms for identification, classification and localization: a brief review of methods." *Journal of The Institution of Engineers (India): Series B*, pp. 1-23, Aug. 2021, doi: 10.1007/s40031-020-00530-0.

[10] S. Devi, N. K. Swarnkar, S. R. Ola and O. P. Mahela, "Detection of transmission line faults using discrete wavelet transform," 2016 Conference on Advances in Signal Processing (CASP), Pune, India, 2016, pp. 133-138, doi: 10.1109/CASP.2016.7746152.

[11] M. Jamil, S. K. Sharma, and R. Singh. "Fault detection and classification in electrical power transmission system using artificial neural network." *SpringerPlus*, vol. 4, no. 1, pp. 1-13, June. 2015, doi: 10.1186/s40064-015-1080-x.

[12] M. N. M. Salleh, N. Talpur, and K. Hussain. "Adaptive neuro-fuzzy inference system: Overview, strengths, limitations, and solutions." In *Data Mining and Big Data: Second International Conference, DMBD 2017, Fukuoka, Japan, July 27–August 1, 2017, Proceedings 2*, pp. 527-535. Springer International Publishing, 2017.

[13] M. J. B. Reddy and D. K. Mohanta, "Performance Evaluation of an Adaptive-Network-Based Fuzzy Inference System Approach for Location of Faults on Transmission Lines Using Monte Carlo Simulation," in IEEE Transactions on Fuzzy Systems, vol. 16, no. 4, pp. 909-919, Aug. 2008, doi: 10.1109/TFUZZ.2008.924210.

[14] M. Paul and S. Debnath, "ANFIS based single line to ground fault location estimation for transmission lines," Michael Faraday IET International Summit 2020 (MFIIS 2020), Online Conference, 2020, pp. 69-74, doi: 10.1049/icp.2021.1077.

[15] Yao Zhang, Qingchao Zhang, Wennan Song, Yixin Yu and Xiao Li, "Transmission line fault location for double phase-to-earth fault on non-direct-ground neutral system," in IEEE Transactions on Power Delivery, vol. 15, no. 2, pp. 520-524, April 2000, doi: 10.1109/61.852978.

[16] O. E. Obi, O. A. Ezechukwu, C. N. Ezema ''An Extended ANN-Based High-Speed Accurate Transmission Line Fault Location For Double Phase To- Earth Fault On Non-Direct-Ground'' *International Journal of Engineering Science Technologies*, vol. 1, no. 1, Jan. 2017, doi: 10.29121/IJOEST.v1.i1.2017.04.

[17] I. Abdulrahman, "MATLAB-Based Programs for Power System Dynamic Analysis," in *IEEE Open Access Journal of Power and Energy*, vol. 7, pp. 59-69, 2020, doi: 10.1109/OAJPE.2019.2954205.

[18] P. Anderson and A. Fouad, Power System Control and Stability, 2nd ed.New Delhi, India: Wiley, 2003.

[19] P. Sauer, M. A. Pai, and J. H. Chow, Power System Dynamics and Stability,2nd ed. Hoboken, NJ, USA: Wiley, 2017.

[20] J. . -S. R. Jang, "ANFIS: adaptive-network-based fuzzy inference system," in IEEE Transactions on Systems, Man, and Cybernetics, vol. 23, no. 3, pp. 665-685, May-June 1993, doi: 10.1109/21.256541.

[21] The MathWorks, Inc. (2022). *MATLAB version: 9.7.0 (R2019b)*.

[22] J. Vesanto and E. Alhoniemi, "Clustering of the self-organizing map," in *IEEE Transactions on Neural Networks*, vol. 11, no. 3, pp. 586-600, May 2000, doi: 10.1109/72.846731.

[23] I. M. Karmacharya and R. Gokaraju, "Fault Location in Ungrounded Photovoltaic System Using Wavelets and ANN," in IEEE Transactions on Power Delivery, vol. 33, no. 2, pp. 549-559, April 2018, doi: 10.1109/TPWRD.2017.2721903.

[24] M. Bhatnagar, A. Yadav and A. Swetapadma, "A Resilient Protection Scheme for Common Shunt Fault and High Impedance Fault in Distribution Lines Using Wavelet Transform," in *IEEE Systems Journal*,

vol. 16, no. 4, pp. 5281-5292, Dec. 2022, doi: 10.1109/JSYST.2022.3172982.
[25]C. H. Kim and R. Aggarwal, "Wavelet transforms in power systems. Part 1: General introduction to the wavelet transforms," *Power Eng. J.*, vol. 14, no. 2, pp. 81–87, Apr. 2000, doi: 10.1049/pe:20000210.
[26]F. Martin and J. A. Aguado, "Wavelet-based ANN approach for transmission line protection," in *IEEE Transactions on Power Delivery*, vol. 18, no. 4, pp. 1572-1574, Oct. 2003, doi: 10.1109/TPWRD.2003.817523.
[27]N. Lightowler, H. Nareid, "Artificial neural network based control systems". SAE transactions, pp. 539-43, Jan. 2003.
[28]C.C Hsu, "Generalizing self-organizing map for categorical data," in *IEEE Transactions on Neural Networks*, vol. 17, no. 2, pp. 294-304, March 2006, doi: 10.1109/TNN.2005.863415.
[29]M. J. B. Reddy and D. K. Mohanta, "Performance Evaluation of an Adaptive-Network-Based Fuzzy Inference System Approach for Location of Faults on Transmission Lines Using Monte Carlo Simulation," in *IEEE Transactions on Fuzzy Systems*, vol. 16, no. 4, pp. 909-919, Aug. 2008, doi: 10.1109/TFUZZ.2008.924210.
[30]S. Kanwal and S. Jiriwibhakorn, "Artificial Intelligence based Faults Identification, Classification, and Localization Techniques in Transmission Lines-A Review," in *IEEE Latin America Transactions*, vol. 21, no. 12, pp. 1291-1305, Dec. 2023, doi: 10.1109/TLA.2023.10305233.
[31]S. Jiriwibhakorn, "Critical Clearing Time Prediction for Power Transmission Using an Adaptive Neuro-Fuzzy Inference System," in *IEEE Access*, vol. 11, pp. 142100 - 142110, Dec. 2023, doi: 10.1109/ACCESS.2023.3341968.
[32]N. A. M. Leh, F. M. Zain, Z. Muhammad, S. A. Hamid and A. D. Rosli, "Fault Detection Method Using ANN for Power Transmission Line," *2020 10th IEEE International Conference on Control System, Computing and Engineering (ICCSCE)*, Penang, Malaysia, 2020, pp. 79-84, doi: 10.1109/ICCSCE50387.2020.9204921.
[33]J.Tian, H.A.Michael, and P.Michael, "Anomaly detection using self-organizing maps-based k-nearest neighbor algorithm." In *PHM society European conference*, vol. 2, no. 1. 2014.
[34]Z.I.Sobhuza, and B. A. Thango. "Study of Fault Detection on a 230kV Transmission Line Using Artificial Neural Network (ANN)." In *2023 31st Southern African Universities Power Engineering Conference (SAUPEC)*, pp. 1-6. IEEE, 2023.
[35]V.Veerasamy, N.I. Abdul Wahab, R. Ramachandran, M. Thirumeni, C. Subramanian, M. Lutfi Othman, and Hashim Hizam. "High-impedance fault detection in medium-voltage distribution network using computational intelligence-based classifiers." *Neural Computing and Applications* 31 (2019): 9127-9143.

S. KANWAL (Student Member, IEEE) received her B.S. and M.Sc degree in electronics from Sir Syed University of Engineering and Technology, Karachi, Pakistan, and King Mongkut's University of Technology, North Bangkok, Thailand, respectively. She is working towards a D.Eng. degree in electrical engineering at the School of Engineering, King Mongkut's Institute of Technology Ladkrabang (KMITL).
Her interests include artificial intelligence-based fault analysis in transmission lines.

S. JIRIWIBHAKORN (Member, IEEE) received his B.Sc. and M.Sc. degrees in electrical engineering from King Mongkut's Institute of Technology Ladkrabang (KMITL), Bangkok, Thailand, in 1994 and 1997, respectively, and his Ph.D. degree in electrical engineering from Imperial College London, UK, in 2000.
He was an associate professor from 2006 to present at the Department of Electrical Engineering, School of Engineering, KMITL. His research interests include power system stability, optimization, planning and forecasting, and applications of neural networks and ANFIS in power engineering.